International Science and Technology Journal
المجلة الدولية للعلوم والتقنية

عدد خاص بالمؤتمر الليبي الدولي للعلوم التطبيقية و الهندسية دورته الثانية
LICASE -2
2024 / 10 / 30-29

المجلة الدولية للعلوم والتقنية
ISTJ

تم استلام الورقة بتاريخ:2024/9/15م وتم نشرها على الموقع بتاريخ: 30/ 10/2024م

The Effect of Activated Flux in TIG Welding Process on the Quality of Weld Geometry of Austenitic Stainless Steel

http://www.doi.org/10.62341/hana0658

Haitem. A. Kushlaf [1*], Hesham Eldghaies [2], Nuri. M. Bhieh [3], Ibrahim. K. Husain [4]
1, 2, 4- The Libyan Advanced Center of Technology, Tripoli, Libya

3 -The Libyan Higher Technical Center for Training & Production, Janzour Libya

* Email: heitemkushlaf@gmail.com

Abstract

Active flux welding (A-TIG) is a method that effectively enhances performance and improves penetration in TIG welding by applying a layer of activated flux to the workpiece before welding. The addition of flux results in higher temperatures in the welding arc, leading to increased penetration without the need for multiple passes and groove preparation, thereby significantly boosting productivity. This research explores the impact of various active fluxes (MoO_3, Cr_2O_3, Fe_2O_3, Al_2O_3, and CaF_2) in A-TIG welding on 6mm thick austenitic stainless steel 304L plates. The investigation focused on surface appearance, weld bead geometry quality, hardness, microstructure, and angular distortion. The findings revealed that utilizing A-TIG welding with Cr_2O_3, MoO_3, and Fe_2O_3 fluxes notably improved the penetration depth and aspect ratio as well as reduced angular distortion compared to conventional (TIG) welding method. The application of fluxes had a minimal impact on the hardness and microstructure of A-TIG weld metal.

Keywords: Activated fluxes (A-TIG), Weld Penetration, Angular distortion, Weld Bead Geometry.

International Science and Technology Journal
المجلة الدولية للعلوم والتقنية

عدد خاص بالمؤتمر الليبي الدولي للعلوم التطبيقية و الهندسية دورته الثانية
LICASE -2
2024 / 10 / 30-29

المجلة الدولية للعلوم والتقنية
ISTJ

تم استلام الورقة بتاريخ:2024/9/15م وتم نشرها على الموقع بتاريخ: 30/ 10/2024م

تأثير الاكاسيد النشطة باستخدام طريقة لحام (TIG) على جودة شكل وابعاد وصلة اللحام للصلب الاوستنيتى المقاوم للصدأ

هيثم كشلاف[*1]، هشام الدغيس [2]، نوري بحيح [3]، ابراهيم حسين [4]

1، 2، 4 المركز الليبي المتقدم للتقنية، طرابلس، ليبيا، 3 المركز الليبي التقني العالي للتدريب والإنتاج، جنزور، ليبيا

الملخص

تعتبر طريقة اللحام باستخدام الأكاسيد النشطة (A–TIG) احدى اهم الطرق التي تعمل على تحسين الأداء والاختراق بشكل فعال في لحام TIG وذلك من خلال تطبيق طبقة من الاكاسيد على قطعة العمل قبل اللحام. تؤدي إضافة الاكاسيد إلى ارتفاع درجات الحرارة في قوس اللحام، مما يؤدي إلى زيادة الاختراق دون الحاجة إلى عمل مسارات متعددة او إعداد شطف لوصلة اللحام، وبالتالي تعزيز الإنتاجية بشكل كبير. يستكشف هذا البحث تأثير مجموعة من الاكاسيد (MoO_3، Cr_2O_3، Fe_2O_3، Al_2O_3، وCaF_2) في لحام A–TIG على ألواح الفولاذ المقاوم للصدأ الأوستنيتي 304L بسماكة 6مم على كل من مظهر السطح وجودة ابعاد درزة اللحام والصلابة والبنية المجهرية والتشوه الزاوي. كشفت النتائج أن استخدام طريقة اللحام (A–TIG) مع الاكاسيد (Cr_2O_3 وMoO_3 وFe_2O_3) أدت إلى زيادة عمق الاختراق ونسبة العمق إلى العرض بشكل ملحوظ بالإضافة إلى تقليل التشوه الزاوي مقارنة بطريقة اللحام (TIG) التقليدية. في حين كان لاستخدام الاكاسيد تأثير ضئيل على الصلابة والبنية المجهرية لمعدن اللحام A–TIG.

الكلمات المفتاحية –اللحام بالأكاسيد النشطة (A–TIG)، عمق اللحام، التشوه الزاوي، ابعاد درزة اللحام.

Introduction

Austenitic stainless steels are widely accepted in the stainless steel family due to their unique properties, such as high strength, ductility, and corrosion resistance. Therefore, they are widely used in various industries. Notably, stainless steels exhibit excellent weldability, allowing them to be joined using various welding techniques, including resistance welding, arc welding, electron beam welding, laser beam welding, friction welding, and brazing. The most popular method of welding austenitic stainless steel is gas tungsten arc welding (GTAW), which is also referred to as tungsten inert gas welding (TIG). It involves melting and joining metals by heating them with an arc formed by a non-consumable tungsten electrode and a workpiece in the presence of a shielding gas [1]. Although TIG welding produces high-quality weld, it is limited to weld thin sheets (2–3mm) in a single pass. Thus, its productivity is relatively low. Thicker weld joints require multiple passes, edge preparation, and filler metal [2]. However, TIG welding has many potentials if productivity can be improved. In terms of time and cost savings, increasing productivity provides a considerable economic advantage to the welding fabrication process. To

تم استلام الورقة بتاريخ:2024/9/15م وتم نشرها على الموقع بتاريخ: 30/ 10/2024م

achieve these goals, a variant of the TIG welding technique, namely (A-TIG), was invented in the 1960s by the E. O. Paton Electric Welding Institute in Ukraine. The idea was to add a thin layer of activating flux, mainly oxides, fluorides, and halides, by mixing them with acetone, methanol, or ethanol to form a smooth paste. By using a soft brush, the flux paste was applied to the joint surface prior to welding. The application of the flux make it possible to intensify the normal TIG welding process, enabling the penetration capability to reach up to 12mm in a single pass. In addition, no edge preparation time or filler wire addition is required. Therefore, low cost and timesaving were offered, which further improve productivity [3]. As well as, improving the mechanical properties and microstructure of the welds [4, 5]. Several researchers have used A-TIG welding and achieved a great improvement in penetration depth. TIG welding using Cr_2O_3 flux significantly increased the aspect ratio of 316L stainless steel welds because A-TIG welding reduces the heat input per unit length of the welds [6]. The performance values of AISI 304 stainless steel plate-welded joints using A-TIG welding have created a full penetration with a good weld appearance without groove preparation of 8mm thickness. Activated flux powder in TIG welding can enhance the ferrite content in the weld metal but does not affect the microstructure of the A-TIG weld [7]. The effect of flux oxides such as Cr_2O_3, Fe_2O_3, MoO_3, SiO_2, and Al_2O_3 on SS 304. Except for Al_2O_3, all other flux oxides exhibit good penetration capability [8]. The results of A-TIG welds using single-component fluxes and multi-component fluxes in 8mm thick austenitic stainless steel plates (AISI 316L) showed that fluxes increase weld penetration. Micro hardness tests revealed the weld zone was stiffer than the base metal, and an increase in delta ferrite content was detected in A-TIG weld zones compared to the base metal [9]. The effects of using different fluxes like Cr_2O_3, SiO_2, TiO_2, MnO_2, and MoO_3 on weld appearance, depth of penetration, bead width, depth/width ratio, and ferrite content using SS2205 duplex stainless steel welded by the TIG process. Experimental investigation revealed that the use of SiO_2 and TiO_2 as fluxes provides greater penetration depth and D/W ratio than other fluxes. In addition, there has been no discernible change in measured micro hardness [10]. The purpose of this study is to investigate the effect of various fluxes and compare them to conventional TIG welding on weld bead geometry, micro hardness, microstructure, and angular distortion.

Material and Methods

In the current experimental study, the metallic material selected is the AISI 304L austenitic stainless steel. This type of steel is widely utilized in various fabrication processes due to its favorable properties. Table 1 shows the chemical composition of the alloy.

International Science and Technology Journal
المجلة الدولية للعلوم والتقنية
عدد خاص بالمؤتمر الليبي الدولي للعلوم التطبيقية و الهندسية دورته الثانية
LICASE -2
2024 / 10 / 30-29
المجلة الدولية للعلوم والتقنية
ISTJ
تم استلام الورقة بتاريخ:2024/9/15م
وتم نشرها على الموقع بتاريخ: 30/ 10/2024م

Table 1. Chemical composition of AISI 304L

C	Mn	Si	Cr	Ni	S	P	Cu	Mo	W	Al	Fe
0.0242	1.42	0.332	17.9	8.24	0.0005	0.0194	0.304	0.293	0.0484	0.0010	Bal

Samples with 6mm thick AISI 304L austenitic stainless steel plates were used in welding experiments with dimensions 100mm x 30mm and 70mm x 150mm. Prior to the welding, the surface of the plate was polished using 400 grit abrasive paper to remove any surface contamination and then cleaned by acetone. The study incorporated the use of activated fluxes including Cr_2O_3, Fe_2O_3, MoO_3, Al_2O_3, and CaF_2. Each flux was prepared in powder form, and then mixed with ethanol, and a thin layer of 0.2mm thick was uniformly applied to the centre line of the surface to be welded using paintbrush. Figure 1 explains the sequences of flux preparation on weld coupon.

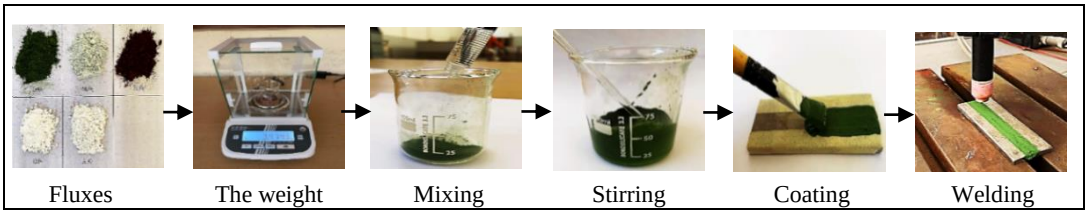

Figure 1. The preparation procedures of A-TIG welding

ESAB 450 PROTIG welding machine with A25 modular component system for mechanized TIG welding was used in the experiments. Based on literature review and experiences, the research carried out multiple welding trials to identify the operating range of welding input parameters as shown in Table 2.

Table 2. TIG welding Process parameters

Polarity	DCEN
Welding current Range	(160 – 200) Amp
Arc voltage Range	(15 – 17) V
Travel speed Range	(90 – 130) mm/min
Electrode and Diameter of Electrode	Thoriated 2% & 2.4mm
Electrode angle tip	45˚
The gap of electrode	3mm
Shielding gas Range	pure argon (99.999) %
Gas flow rate	(8 – 16) L/min
Inclination electrode angle	90˚
Electrode extension	5mm
Nozzle diameter	8mm

The welding process was applied to examine the effect of various fluxes on weld bead geometry. After welding, a visual inspection was performed to assess the effect of activating fluxes on the surface appearance. The samples were etched by a solution

تم استلام الورقة بتاريخ:2024/9/15م وتم نشرها على الموقع بتاريخ: 30/ 10/2024م

containing 15ml of hydrochloric acid (HCL), 5ml of nitric acid (HNO_3), and 10ml of glycerine to expose the weld shape. The cross-sections of the weld beads were photographed using an optical microscope (Nikon), followed by a micro hardness test and microscopic examination. Furthermore, samples were prepared for assessing the angular distortion test using the grid technique as shown in Figure 2(a). Prior to welding, equal distances were marked on the surfaces of the plates and carefully aligned on a level surface and inspected to identify any inconsistencies. Vertical displacement measurements were taken at three points before welding to evaluate any variations that could affect the joint, and the average value was recorded, as shown in Figure 2(b).

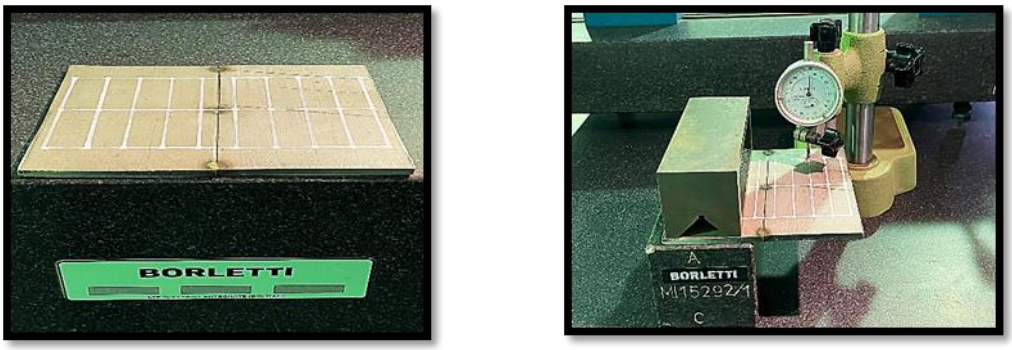

(a) (b)

Figure 2. (a) The grid technique; (b) angular distortion measurement

After welding, the angular distortion Θ is calculated as shown in Figure 2(c), the vertical displacement value for each position divided by half the width of the main plate and given by the following equation؛

$\Theta = \tan^{-1} (\Delta Z/\Delta X)$

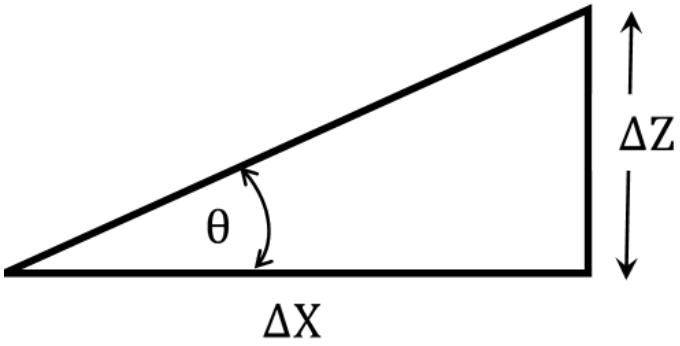

Figure 2. (c) Schematic diagram of angular distortion measurements

International Science and Technology Journal
المجلة الدولية للعلوم والتقنية
عدد خاص بالمؤتمر الليبي الدولي للعلوم التطبيقية و الهندسية دورته الثانية
LICASE -2
2024 / 10 / 30-29
المجلة الدولية للعلوم والتقنية
ISTJ
تم استلام الورقة بتاريخ:2024/9/15م
وتم نشرها على الموقع بتاريخ: 30/ 10/2024م

Results and Discussion

Effect of fluxes on the appearance of the weld surface

Figure 3 shows the specimen surfaces of TIG welding without flux and with various fluxes at the operating welding condition. Figure 3(a) shows the results of the welds without flux, which produced a smooth, clean, and spatter-free surface appearance due to no flux being applied to it. Figure 3(b, c, d, e, f) demonstrates the flux effect of Cr_2O_3, MoO_3, Fe_2O_3, Al_2O_3, and CaF_2 respectively, showing an acceptable formation of residual slag and spatter. The results indicated that TIG welds produced with oxide fluxes contributed to forming the residual slag. However, the intensity of residual slag and spatter can be attributed to many factors, such as the thermosphysical properties of the flux, i.e. melting and boiling point, chemical composition, grain size of the deposit flux layer on the metal surface prior to the welding, the welding mode conditions, and the parameters [11].

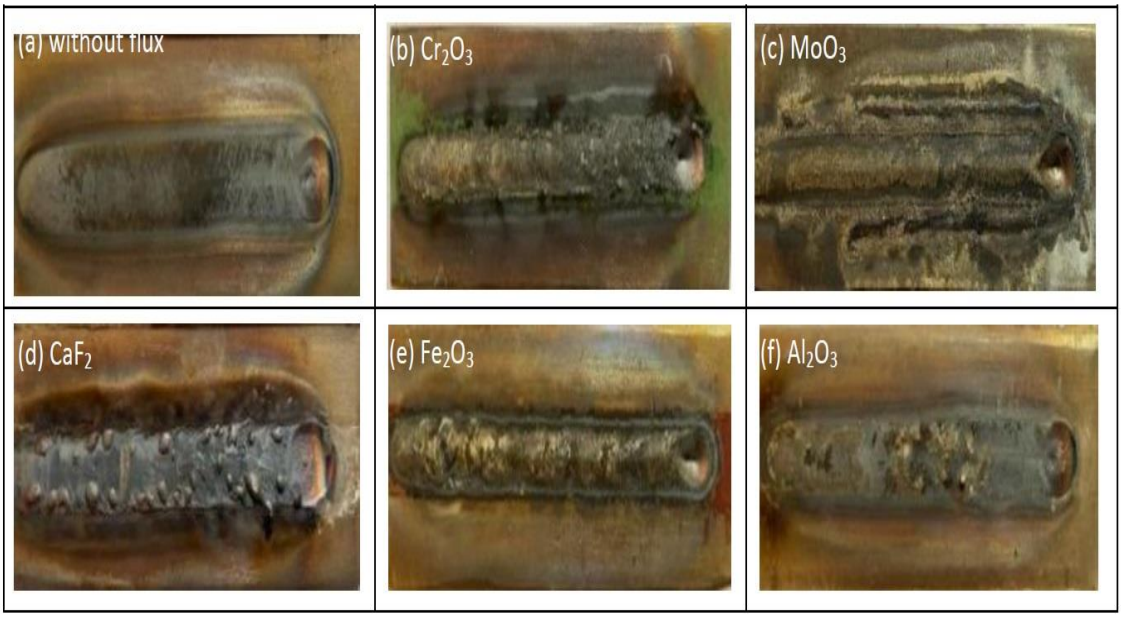

Figure 3. Effect of A-TIG welding with different flux powders on the surface appearance

Effect of flux on weld bead geometry

The D/W ratio is used to quantify variations in weld bead shape, which is a key factor in determining the quality of the welding. Figure 4 illustrates the effect of different fluxes on the weld bead geometry by contrasting the depth of penetration, weld bead width, and depth-to-width ratio.

تم استلام الورقة بتاريخ:2024/9/15م وتم نشرها على الموقع بتاريخ: 30/ 10/2024م

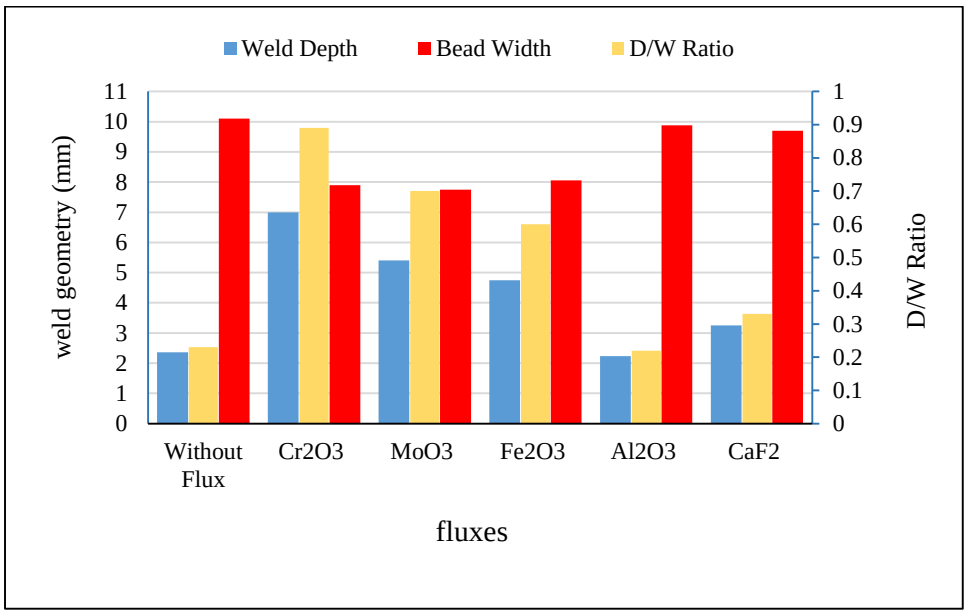

Figure 4. Comparison of activating fluxes on weld bead geometry

The macrostructure of weld bead geometry of TIG and A-TIG with various fluxes (on 6mm thick stainless steel 304L plates) was measured according to the width and depth of the welds as shown in Figure 5. Under identical operating parameters obtained of 180amps current, 110mm/min weld speed, and gas flow rate of 10L/min. TIG welds without flux exhibited a wide and shallow morphology Figure 5(a). TIG welds with flux, which is composed of Cr_2O_3, MoO_3, and Fe_2O_3, powders, exhibited a narrow and deep morphology Figure 5(b, c, d). The highest penetration 7.0mm alongside a bead width of 7.9mm and a peak value of D/W ratio (0.89) is reported with Cr_2O_3 flux as depicted in Figure 5(b). This can be attributed to the strong arc constriction and reversal of Marangoni convection mechanisms. This result is 197% more than conventional TIG. MoO_3 and Fe_2O_3 fluxes also demonstrate an increase in D/W (0.7 and 0.6), exhibiting an increase of 129% and 101% respectively, compared with conventional TIG. Whereas, using CaF_2 flux showed a slight increase in penetration depth up to 38%. The Al_2O_3 flux caused a slight deterioration in penetration depth by (2.23mm) compared to 2.36mm with conventional TIG.

The geometries of the welds vary between the TIG and A-TIG welding techniques. Current research indicates that the surface tension gradient and plasma arc column play a significant role in improving the penetration of an activated TIG weld. The fundamental concept involves reversing the fluid flow direction due to a reversal in the relationship between temperature and surface tension. In TIG welding, the molten metal moves from the center to the edges of the weld pool because the surface tension at the pool's center is lower than at the edges ($\delta\gamma/\delta T < 0$), transferring heat to the pool's edge. Consequently, the welding pool becomes wider and shallower, a phenomenon known as the Marangoni

effect. Conversely, when TIG welding with Cr_2O_3, Fe_2O_3, MoO_3, and CaF_2 fluxes is used, the surface tension gradient ($\delta\gamma/\delta T > 0$) shifts from negative to positive with temperature variations. This alteration causes the fluid flow direction to switch from the pool's boundary to the center, leading to heat transfer toward the core of the pool and resulting in a narrower and deeper weld bead. This process is called the reverse Marangoni effect, as discussed by various researchers [12– 14]. However, the other major mechanism of increasing the depth of penetration is called arc constraction. In this case, the fluxes Cr_2O_3, Fe_2O_3, MoO_3, and CaF_2 decompose under the column temperature and vaporized particles produce positive ions. These ions capture the free electrons in the outer region of the arc, leading to arc constriction. Due to the constricted arc, more melting of base metal and high temperature in the weld pool exist, resulting in a deep penetration [15, 16]. Moreover, oxides appear to have two functions in the activating flux process. The first function is the effect of oxides on the surface chemistry of base metals, where the presence of oxygen in the oxide flux leads to a shift in the surface tension temperature coefficient on the molten pool from negative to positive, resulting in centripetal Marangoni convection mode. The second function is to enhance the arc physics because of the presence and dissolution of oxide on the welding surface and under electrical arc [17, 18].

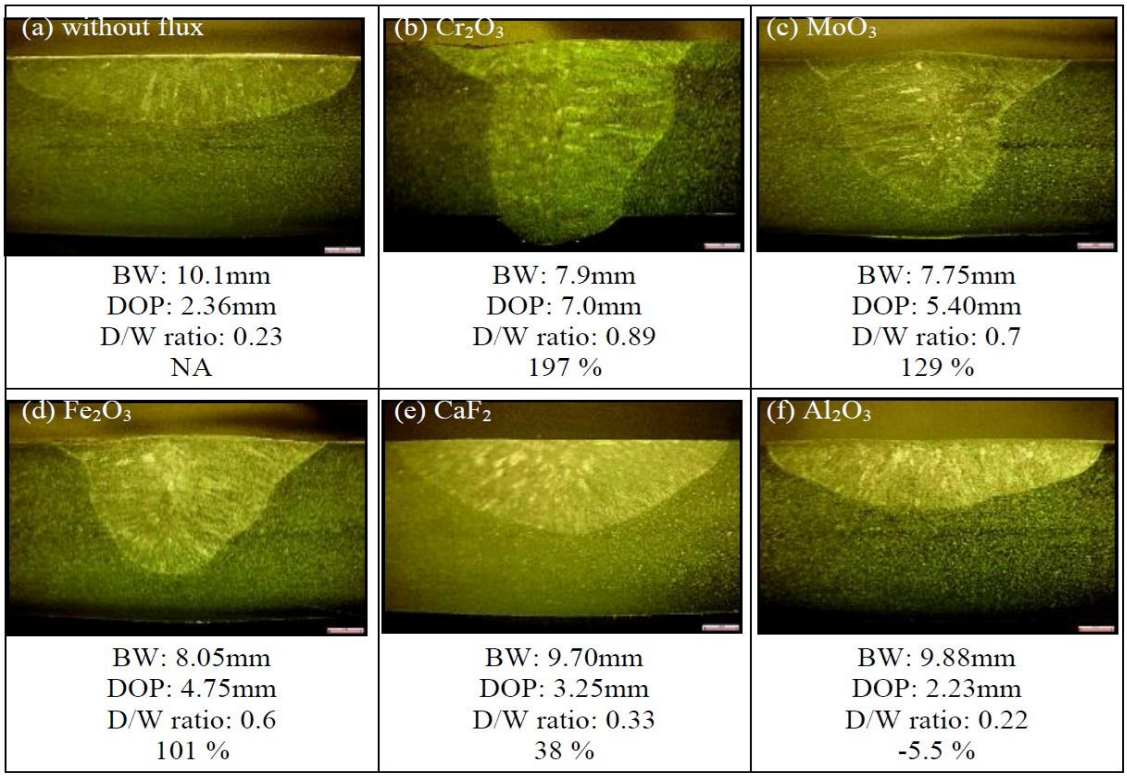

Figure 5. Effect of A-TIG welding with different flux on weld morphology at 2X magnification

Hardness and Microstructure examination of A-TIG process

The effect of different fluxes on micro hardness was examined as shown in Figure 6. According to ASTM E92-82 [19] standard. Vickers micro hardness measurements were made at load of 200g for 10sec on a cross-section specimen at 0.5mm intervals over a span of 5.5mm covering welded zone, heat-affected zone, and the base metal. Results showed varying hardness values for different fluxes and no flux. Fluxes like Cr_2O_3, CaF_2, Al_2O_3, MoO_3, and Fe_2O_3 affected the hardness of weld metals differently. Austenitic stainless steel weldments had varying hardness values compared to the base metal. The addition of flux has a positive effect of increasing the heat input of the welds, leading to form more delta-ferrite and subsequently improved mechanical properties. The hardness results were consistent with previous studies [20– 22], showing no significant differences between base metal and weld metal hardness. Upon examining the results of micro hardness assessment, the microstructure depicted in Figure 7 indicates that there is a negligible disparity in the microstructural configuration of the samples with and without the flux, with the dark delta ferrite phase present in the form of a framework within the austenitic structure. Throughout the cooling process and as a result of solidification, the thinner ferrite layers evolved into austenite; nevertheless, the broader primary dendrites remained partially undissolved, and the central regions of the dendrites containing high chromium and low nickel persisted as skeletal ferrite within the ultimate microstructure [23, 24]. This phenomenon is linked to the thermal energy input utilized; it is widely acknowledged that alterations in the magnitude of the thermal energy input can influence the microstructure.

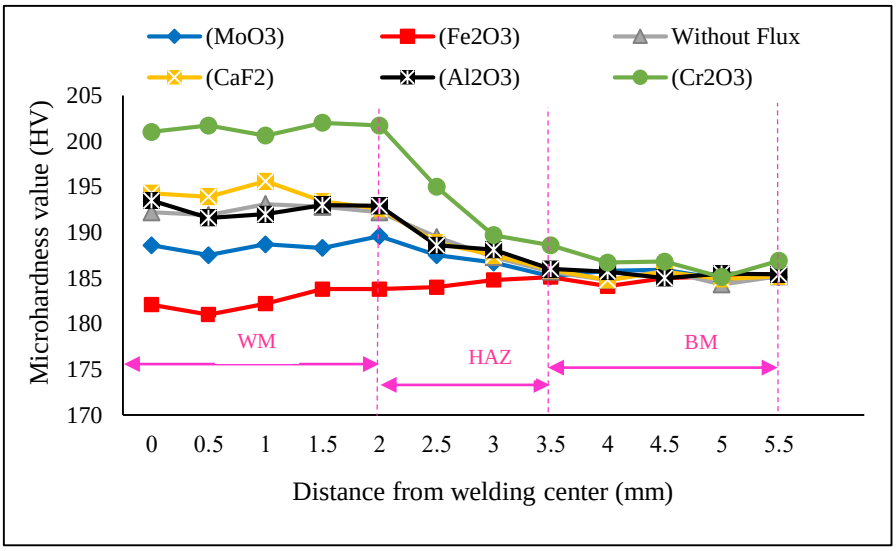

Figure 6. Effects of fluxes on Vickers micro hardness

International Science and Technology Journal
المجلة الدولية للعلوم والتقنية
عدد خاص بالمؤتمر الليبي الدولي للعلوم التطبيقية و الهندسية دورته الثانية
LICASE -2
2024 / 10 / 30-29
تم استلام الورقة بتاريخ:2024/9/15م
وتم نشرها على الموقع بتاريخ: 30/ 10/2024م

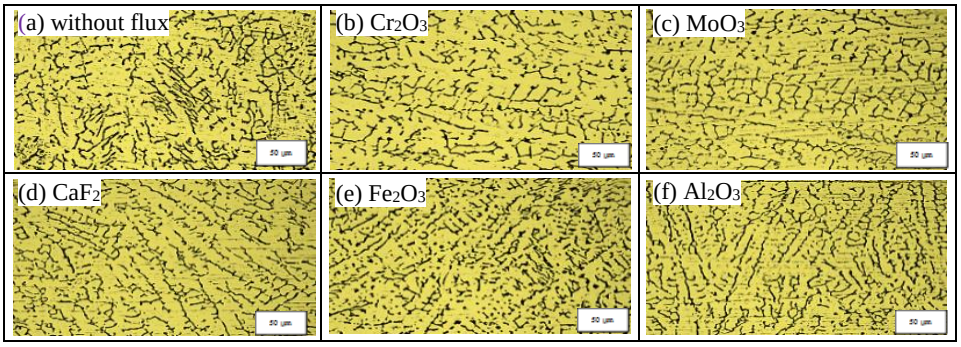

Figure 7. Microstructure of the autogenous TIG welds and A-TIG welds at 400X magnificatio

Effect of fluxes on angular distortion

Angular distortion in welded samples is mainly caused by expansions and contractions that occur in the weld metal and base metal during the welding thermal cycle. As a result, uneven heating along the thickness direction at the weld seam induces non-uniform transverse shrinkage, resulting in angular distortion of the weldment. Several factors can influence angular distortion, such as the depth of penetration and the geometric shape of the weld. As well as the power density of the heat source, which is an important factor for determining the shape of weldment. However, in activated TIG welding, both the penetration depth and depth-to-width ratio can be considerably increased, which implies a higher energy of concentration during welding. This led to a reduction in the amount of heat supplied. Therefore, preventing overheating reduces the angular distortion [25]. Figures 8 and 9 illustrate the effect of conventional TIG and A-TIG with different fluxes on the angular distortion.

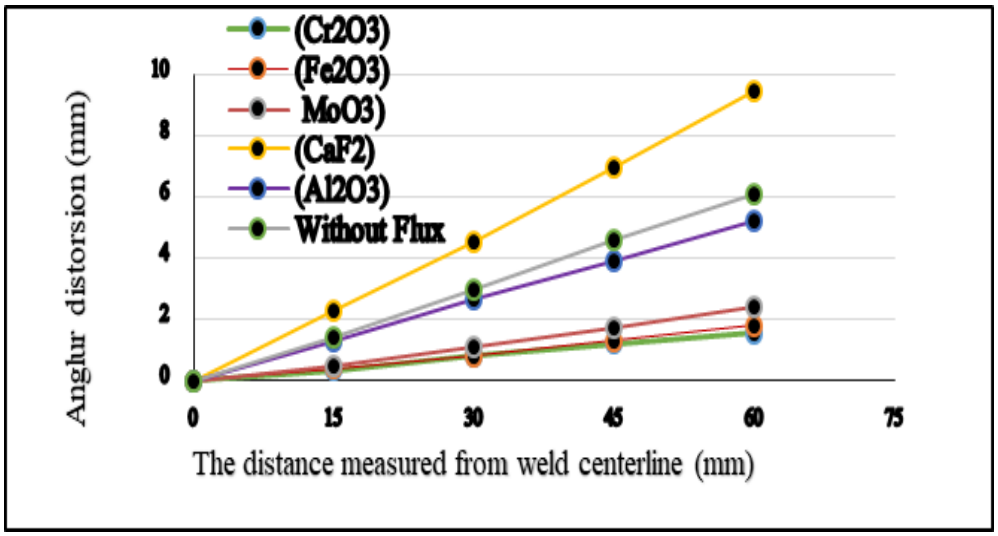

Figure 8. Distribution of angular distortion

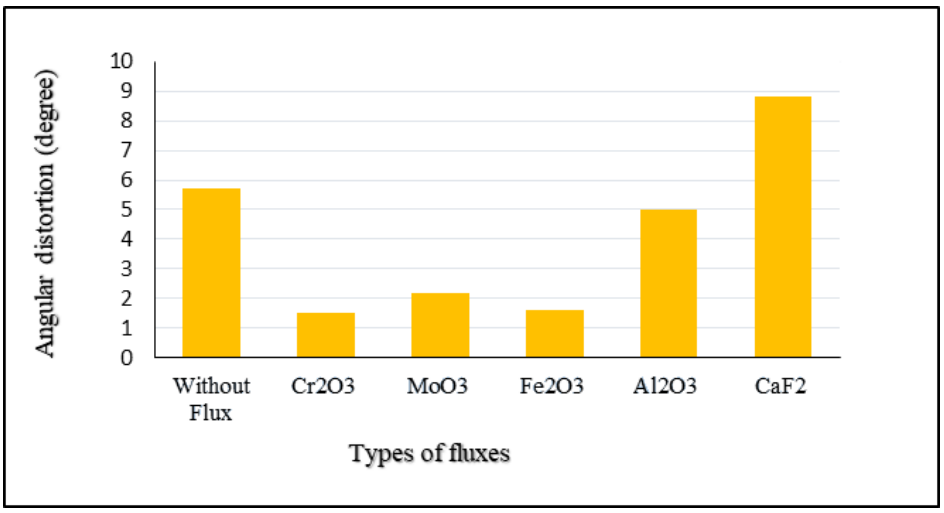

Figure 9. Effect of using flux on angular distortion

It was clear that the lowest value of angular distortion occurred with Cr_2O_3 flux of 1.55mm equal to 1.5˚. In conventional TIG welding, an angular distortion was 6.1mm, 5.7°, while adding CaF_2 flux has raised the angular distortion to the highest value of 9.45mm and 8.8˚. On the other hand, Al_2O_3 flux yields a distortion of 5.2mm with 5.0˚. Whereas, Fe_2O_3 and MoO_3 fluxes notably reduce angular distortion to 1.8mm, 1.6˚, and 2.4mm, 2.2˚, respectively. It is found that Cr_2O_3, Fe_2O_3, and MoO_3 fluxes produce a considerable increase in penetration and aspect ratio, thus enhancing the power density of the heat source, leading to reduce the angular distortion of the weldment.

Conclusion

The main conclusions obtained in this study can be summarized as follows:

a) The surface appearance of the A-TIG welds produces an acceptable formation of residual slag. Whereas, the weld surface of conventional TIG welding is generally smooth and spatter-free.
b) The optimum welding parameters of the A-TIG welding process using Cr_2O_3 flux include a current of 180 Amp, a speed of 110mm/min, and a Gas flow rate of 10 L/min. It had a remarkable effect on the weld bead morphology, which produced a maximum weld penetration of 7 mm and a D/W ratio of 0.89.
c) The maximum depth-to-width ratio achieved with the use of activated fluxes including Cr_2O_3, MoO_3, and Fe_2O_3 are 0.89, 0.7, and 0.6, respectively, and in the case of conventional TIG, it was 0.23. There is an increase in aspect ratio with the Cr_2O_3 flux by 197% compared to the conventional TIG welding process.
d) The impact of flux addition on A-TIG weld metal hardness is not significant. Cr_2O_3 flux results in highest micro hardness in fusion zone, followed by Al_2O_3 and CaF_2, while Fe_2O_3 and MoO_3 fluxes have lower micro hardness than conventional TIG

welding. The microstructure of welded specimens with and without flux remains largely unchanged, with dark delta ferrite phase present in austenite matrix. Addition of fluxes decreases thermal conduction and solidification rate of metal.

e) Angular distortion of the weldment when using A-TIG is reduced compared to conventional TIG welding. This is due to an increase in the depth-to-width ratio, which indicates the presence of arc constriction during the welding process.

References

[1]. Ken-Hicken G. Gas tungsten arc welding. AMERICAN STANDART METALS. ASM handbook, New York (1993): ASM: 580-605.

[2]. Vasudevan M. Effect of A-TIG welding process on the weld attributes of type 304LN and 316LN stainless steels. Journal of materials engineering and performance, 26(3) (2017), pp. 1325-1336.

[3]. Lu S, Fujii H, Sugiyama H, and Nogi K. Mechanism and optimization of oxide fluxes for deep penetration in gas tungsten arc welding. Metallurgical and materials transactions A, 34A (2003), pp. 1901-1907.

[4]. Dhandha, K.H. and Badheka, V.J. Effect of activating fluxes on weld be morphology of P91 steel bead-on-plate welds by flux assisted tungsten inert gas welding process. Journal of Manufacturing Processes, 17 (2015), pp. 48-57.

[5]. Nayee, S. G. and Badheka, V.J. Effect of oxide-based fluxes on mechanical and metallurgical properties of Dissimilar Activating Flux Assisted-Tungsten Inert Gas Welds. Journal of Manufacturing Processes, 16 (2014), pp. 137-143.

[6]. Tseng K.H, Chen Y.C, and Chen K.L. Cr_2O_3 Flux Assisted TIG Welding of Type 316L Stainless Steel Plates. Applied Mechanics and Materials, 121-126 (2012), pp. 2592-2596.

[7]. Liu G.H, Liu M.H and YI Y.Y. Activated flux tungsten inert gas welding of 8 mm-thick AISI 304 austenitic stainless steel. J. Cent. South Univ, 22 (2015), pp. 800-805.

[8]. Kumar. H, Singh N. K. Performance of activated TIG welding in 304 austenitic stainless steel welds. Materials Today: Proceedings, 4(9) (2017), pp. 9914–9918.

[9]. Kulkarni A, Dwivedi D.K, and Vasudevan M. Effect of oxide fluxes on activated TIG welding of AISI 316L austenitic stainless steel. Materials Today: Proceedings, 18 (2019), pp. 4695-4702.

[10]. Nanavati P.K, Badheka V.J, Idhariya J, and Solanki D. Comparisons of Different Oxide Fluxes in Activated Gas Tungsten Arc Welding of Duplex Stainless Steels for Improved Depth of Penetration and Pitting Corrosion Resistance. Advances in Materials and Processing Technologies (2021), DOI: 10.1080/2374068X.2021.1916283.

[11]. Pandya D, Badgujar A, Ghetiya N and Oza A.D. Characterization and optimization of duplex stainless steel welded by activated tungsten inert gas welding process. Int. J. Interact. Des. Manuf, (2022), pp. 1–13.

[12]. Vidyarthy R.S and Dwivedi D.K. Activating flux tungsten inert gas welding for enhanced weld penetration. Journal of Manufacturing Processes, 22 (2016), pp. 211-228.
[13]. Patel D and Jani S. Techniques to weld similar and dissimilar materials by ATIG welding- an overview. Materials and Manufacturing Processes, (2022) DOI: 10.1080/10426914.2020.1802040.
[14]. Ibrahim. K. H, and Hesham E. Influence of Activated Flux TIG Welding on Penetration Improvement of Low Carbon Steel. (AJAPAS), 02 (4) (2023), pp. 224-230.
[15]. Tseng K.H, and Sung H.L. Advances in Fusion Welding Technique of Austenitic Stainless Steels. Engineering Materials, 480-481 (2011), pp. 527-532.
[16]. Singh S.R and Khanna P. A-TIG (activated flux tungsten inert gas) welding: – A review. Materials Today, 44 (2021), pp. 808-820.
[17]. Leconte1 S, Paillard P, Chapelle P, Henrion G and Saindrenan J. Effect of oxide fluxes on activation mechanisms of tungsten inert gas process. Science and Technology of Welding and Joining, 11 (4) (2006), pp. 389-379.
[18]. Yushchenko K.A, Kovalenko D.V, and Kovalenko I.V. Peculiarities of A-TIG welding of stainless steel. Trends in Welding Research, ASM International, (7thed.) (2005), pp. 367-376.
[19]. ASTM E92-82. 1982. Standard Test Method for Vickers Hardness of Metallic Materials.
[20]. Chandrasekar G, Kailasanathan C, Verma D.K, and Nandagopal K. Optimization of Welding Parameters, Influence of Activating Flux and Investigation on the Mechanical and Metallurgical Properties of Activated TIG Weldments of AISI 316L Stainless Steel. Trans Indian Inst Met. (2017). DOI 10.1007/s12666-017-1046-5.
[21]. Tseng K.H, and Chuang K.J. Application of iron-based powders in tungsten inert gas welding for 17Cr–10Ni–2Mo alloys. Powder Technology, 228 (2012), pp. 36-46.
[22]. Tseng K.H and Hsu C.Y. Performance of activated TIG process in austenitic stainless steel welds. Journal of Materials Processing Technology, 211 (2011), pp. 503-512.
[23]. Ma J.C, Yang Y.S, Tong W.H, Fang Y, Yu Y, and Hu Z.Q. Microstructural evolution in AISI 304 stainless steel during directional solidification and subsequent solid-state transformation. Materials Science and Engineering A 444 (2007), pp. 64-68.
[24]. Leone G.L, and Kerr H.W. The Ferrite to Austenite Transformation in Stainless Steels. Welding research supplement. 61 (1982), pp. 13-21.
[25]. Lingyue Z, and Anming Hu. Fe_2O_3 Nanowire Flux Enabling Tungsten Inert Gas Welding of High-Manganese Steel Thick Plates with Improved Mechanical Properties. Appl. Sci. (2021), 11, 5052.